Flow of a vortex-pair street and the evolution of salt fingers

Hie-Tae Moon
Department of Physics, Korea Advanced Institute of Science and Technology, Daeduk Science-town 305-701, Korea
(Received 22 October 1998)

We considered the geometry of a double row of vortex pairs in an ideal fluid, and studied the evolution of salt fingers from the geometry systematically. This study illustrates the mechanism of the generation of large-scale convective cells at the final stage of the fingering instability. We discuss why in the growth of double-diffusive salt fingers the emergence of such large convection cells has been implicated phenomenologically as an onset to turbulence, terminating the finger growth. [S1063-651X(99)12010-5]

PACS number(s): 47.32.Cc, 47.20.Dr, 47.54.+r

''Salt fingers'' refer to the long, thin cells of alternating upward and downward motion found near the surface of a heated ocean. This form of convection was first discussed by Stommel, Arons, and Blanchard in 1956 [1], when it was considered to be an oceanographic curiosity. It is now recognized that salt fingering is a feature of major importance in transport processes in many physical systems [2].

Salt fingers grow at the interface of two uniform fluid layers with different diffusity in a gravitationally stable environment. They can also be two dimensional. In a Hele-Shaw cell, made up, for example, of two glass plates, 50 $\times 50\,\mathrm{cm}^2$, each separated by a 0.1-cm spacer, an initial state consisting of sugar solution lying above a denser salt solution is unstable to disturbances and evolves into long, slender two-dimensional fingers [3,4]. While the evolution of salt fingers is difficult to follow in a regular fluid, the Hele-Shaw configuration does provide a control that is not possible with a regular fluid.

There now exists extensive literature on the salt-finger convection [5–7]. However, an understanding of how the salt fingers evolve is still a matter of considerable difficulty. The study of the finite-amplitude evolution of the fingers is hindered most of all by the complex turbulent process involved.

Double-diffusion and advection, and possibly their interplay, are the key dynamical processes in the growth of salt fingers. It is recognized that double diffusion has an important role to maintain the density profile gravitationally stable so that salt fingers can grow. The major role of the advection, on the other hand, appears not well understood in general. To gain a better perspective of the fingering dynamics, one might then want to suppress the small-scale structures at both the viscous and diffusive scales, and focus only on the advective nature of the salt fingers. This motivates us here to consider the evolution of salt fingers in an inviscid ideal fluid of uniform density. Previous simulations of the complete governing equations for the double-diffusive salt fingers can be found in Refs. [8], [9].

In this study, we consider the flow generated from the street of vortex pairs as shown in Fig. 1, where the vortex pairs forming the street are magnified in the insets. Initially, each vortex pair here consists of a linear array of point vortices, one half of the line having a positive vorticity, the other half having a negative vorticity. To express the initial vorticity configuration, we define a periodic step-function S as follows:

$$S(x;\lambda,\phi)=\frac{\sin\left\{\left(\frac{2\pi}{\lambda}\right)x+\phi\right\}}{\left|\sin\left\{\left(\frac{2\pi}{\lambda}\right)x+\phi\right\}\right|}, \tag{1}$$

where λ and ϕ represent, respectively, the period and the phase of the step function.

Denoting the positions of point vortices by $(x_1,y_1),(x_2,y_2),\ldots$, and their strengths by $\omega_1,\omega_2,\ldots$, the initial configuration of vorticity can now be expressed as

$$(x_n,y_n)=(n\,\delta x,h_0 S(n\,\delta x;\lambda,-\pi/2)),\quad n=1,\ldots,N,$$

$$\omega_n=\kappa S(n\,\delta x;\lambda,-\pi), \tag{2}$$

where δx is an interval between neighboring point vortices, equal to the box size (L) divided by the total number of point vortices ($N=3840$), and $2h_0$ is the thickness of the street of vortex pairs and κ denotes the strength of vorticity. The specific values of the initial phase here are owing to the choice of the origin of the coordinates (cf. Fig. 1).

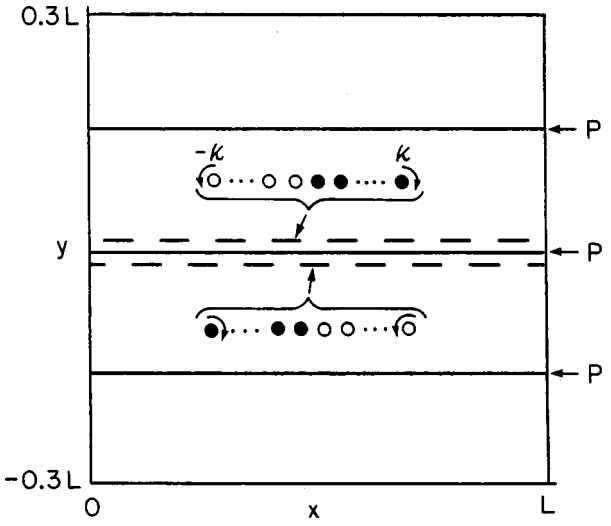

FIG. 1. The initial vorticity configuration. The insets magnify the vortex lines, where a dot denotes a point vortex with positive vorticity κ while a blank denotes a point vortex with strength $-\kappa$. The letter P denotes a line of dyed fluid particles.

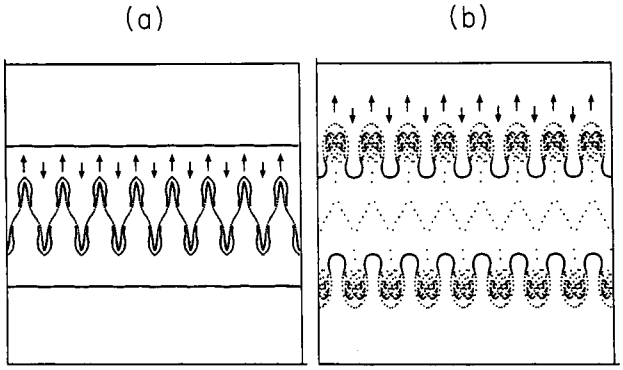

FIG. 2. Evolution of salt fingers from the initial configuration. (a) $t=1.6$ sec. Notice the entrainment of the dyed fluid particles located at $y=0$. (b) $t=9.6$ sec. Now the finger height is about 20 times that of its initial value.

The future vorticity field $\omega(x,y,t)$ is governed by the Euler equation given by

$$\frac{\partial \omega}{\partial t}=\frac{\partial \psi}{\partial x}\frac{\partial \omega}{\partial y}-\frac{\partial \psi}{\partial y}\frac{\partial \omega}{\partial x},$$

$$\left(\frac{\partial^2}{\partial x^2}+\frac{\partial^2}{\partial y^2}\right)\psi=-\omega, \tag{3}$$

where $\psi(x,y,t)$ is the stream function, and the velocities (u, v) of the flow are given, respectively, by the relations $u=\partial\psi/\partial y$, $v=-\partial\psi/\partial x$.

The evolution of the flow field from the given initial configuration of vorticity is not tractable analytically and one has to resort to Eq. (3) numerically for the evolution of the field. The following numerical schemes are employed in this study. For the integration of space, we used the pseudospectral method [10] on the $N_x\,(=128)$ by $N_x\,(=256)$ grids. The initial vorticity on the grid nodes is obtained from the point vortices through the method known as the cloud-in-cell interpolation [11], which smooths the vorticity of a point vortex over four neighboring grid points through a linear area-weighting interpolation. For the time integration, we used the predicting leapfrog scheme followed by a correcting trapezoidal step [12]. The numerical integration will be carried out on the spatial domain $0<x<6.4$ cm and $-6.4<y<6.4$ cm under periodic boundary conditions. $h_0=0.1$ cm and $\kappa=0.2/\text{sec}$ are chosen. As a wavelength of the step function we chose $\lambda=0.8$ cm, which allows 16 fingers to grow in the given box, 8 upward and 8 downward.

To follow the evolution of the flow field more systematically, the flow field will be visualized in this study. For visualization purposes, we place dyed fluid particles at certain locations and track their movements in time. For example, the lines denoted by the letter P in Fig. 1 are dyed fluid particles distributed for such purpose.

Evolution of salt fingers in an ideal fluid

We see in Fig. 2 that long slender fingers are generated at the interface between the upper $(y>0)$ and the lower $(y<0)$ fluids. We observe here that the fingers evolve with a leading end forming an oval consisting of two equal and opposite vortices that penetrates into the fluid above and below. Notice the entrainment of the dyed fluid particles located at $y=0$. The particular portion of the fluid entrained within the leading oval of the finger accompanies the oval in its career. It can be seen in Ref. [8] that the finger tips of double-diffusive salt fingers are indeed made of a pair of counter-rotating vortices.

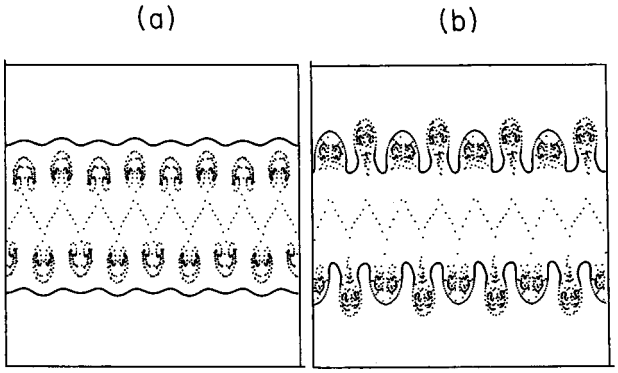

FIG. 3. Characteristic instability of the fingers for the subharmonic perturbation in phase, (a) $t=3.9$ sec, (b) $t=9.3$ sec.

The height of the fingers in Fig. 2(b) is now about 20 times that of the initial height, and the fingers are expected to continue to grow as if there were no perturbations interfering. This result confirms the evolution of fingers in an ideal fluid from the given initial geometry.

Subharmonic perturbation in phase

Next, we add a subharmonic perturbation to the initial configuration of vorticity:

$$\omega_n'=\omega_n\{1+0.05S(n\,\delta x;2\lambda,-\pi/4)\},\quad n=1,\ldots,N, \tag{4}$$

where 2λ is the wavelength of the subharmonic perturbation. The perturbation is such that the strengths of every other vortex pair are now strengthened by 5%, while the rest are weakened by 5%.

The corresponding evolution is visualized in Fig. 3, where we see that the growth of salt fingers is unstable and the finger structures form alternatingly tall and short. The fingers that are taller and slimmer correspond to the strengthened vortex-pairs.

Subharmonic perturbation out of phase

Here we apply the same subharmonic perturbation but out of phase by $\pi/4$ with respect to the previous subharmonic one:

$$\omega_n'=\omega_n\{1+0.05S(n\,\delta x;2\lambda,-\pi/2)\},\quad n=1,\ldots,N. \tag{5}$$

Under this perturbation, each of the vortex pairs is now *asymmetric* in that one of the paired vortices is strengthened by 5% while the other is weakened by 5%. The vortex pairs therefore tend to rotate to the side of higher strength as they move. Since the perturbation is subharmonic with wavelength 2λ, every other vortex pair in the upper row, for example, may rotate clockwise as they move up while the rest

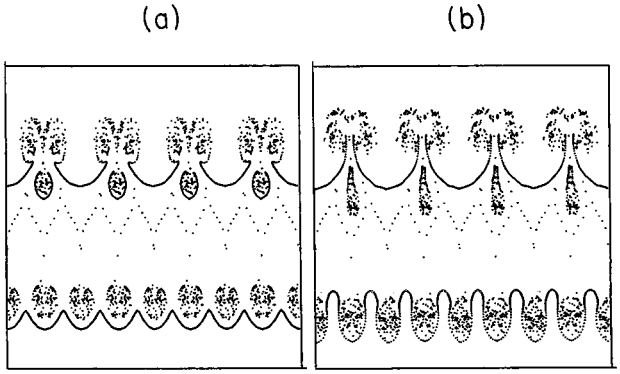

FIG. 4. Characteristic instability of the fingers for the subharmonic perturbation out of phase. Only the upper row is perturbed. (a) $t=12$ sec. Immediately after the collision. (b) $t=15$ sec. An array of large-scale convective overturning is generated in the upper reservoir. At the same time, an array of small vortex pairs is generated that move back into the finger region.

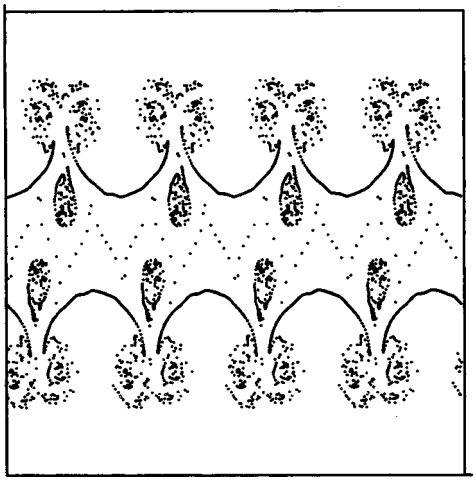

FIG. 5. Characteristic instability for the subharmonic perturbation out of phase. Both rows are perturbed. $t=13.2$ sec.

rotate in opposite direction as they move up. The fingers therefore will collide with the neighbor eventually as they move up.

In Fig. 4, we perturbed the upper row only for clarity, where we see that as the ascending finger tips collide, an array of large-scale overturning convective cells emerge in the upper reservoir. At the same time, we see the emergence of an array of small-scale vortex-pairs that move down fast back into the finger region. The lower row, not perturbed initially, generates an array of salt fingers that continue to penetrate into the reservoir below. When both rows are perturbed (Fig. 5), each row now develops into an array of large-scale overturning convective structures in the reservoir and an array of small vortex pairs moving fast backward into the finger zone.

The dynamical significance of the collision of the finger tips can be outlined as follows. First, the collided finger tips, now detached from the fingers, give rise to a large-scale overturning of the flow, which blocks the growth of the fingers underneath. In Fig. 4(b), we see that the large-scale overturning of the flow in the upper reservoir actually reduces the height of the fingers to a value less than half of the height of the unperturbed fingers that grow in the lower region. Second, in the mean time, the concomitant small vortex pairs that move fast back into the finger zone actually destroy the fingers left within the finger zone. This result is consistent with the phenomenology that the appearance of the large convective cells at the reservoirs implicates the onset of turbulence, terminating the finger growth.

The trace of such mushroom-type cells of convective overturning in the double-diffusive salt fingers can actually be found in previous simulations including both diffusion and viscosity [9], where it was argued that such a structure seemed to be a robust dynamical result. This study illustrates that the large-scale convective overturning results from the collision of finger tips and should be accompanied by a small vortex pair moving in opposite direction. Clearly, some of the ascending fluids along the upward fingers can change their direction after the collision and are carried back into the finger region by the smaller vortex pairs. This result further implicates that, in the actual double-diffusive fingering instability, the finger region invaded by the concomitant small vortex pairs would become hydrostatically unstable, where finger structures are unstable and turbulence takes place.

Next, we provide an explanation for the mechanism of the generation of the large-scale convective overturning. To this

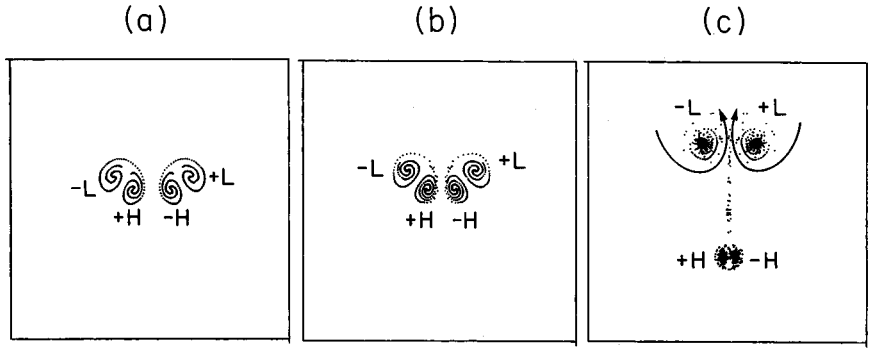

FIG. 6. The collision of two *asymmetric* vortex pairs ascending. H denotes a vortex with higher strength, while L denotes one with lower strength. $+$ indicates the clockwise sense while $-$ stands for the counterclockwise sense. (a) Two ascending vortex pairs are about to collide. (b) At the moment of collision, a part of the pair is being exchanged to satisfy the continuity of the flow. (c) After the collision, $+H$ and $-H$ combine tightly to form a new small vortex pair moving quickly downward. Leaving behind is a slowly ascending pair of now *distanced* $+L$ and $-L$, which entrains neighboring fluids as indicated by arrows, creating a large-scale convective overturning of the flow.

end, we show in Fig. 6 a critical collision process of two asymmetric vortex pairs as they ascend. At the moment of collision [cf. Fig. 6(b)], a part of the vortex pairs is exchanged. The part with higher vorticity, denoted by $+H$ or $-H$, combines tightly to form a new vortex pair that moves quickly downward, leaving behind a pair of vortices with lower intensity, $+L$ and $-L$, which ascends only slowly compared to the $+H$ and $-H$ pair. Such an exchange is necessary in order to satisfy the continuity of the flow. The pair of now *distanced* counter-rotating vortices, the $+L$ and $-L$ pair, is much larger in size and entrains the neighboring fluids in the reservoir *into* the center region of the pair and then pushes them up, as indicated by arrows in Fig. 6(c). In this way, the large-scale overturning of the flow is created in the reservoir.

We conclude this study with the following remarks. This study is concerned with the evolution of salt fingers from the street of vortex pairs in an ideal fluid. It has been demonstrated that the formation of coherent vortices and their interactions are of fundamental importance in the dynamics of salt fingers. The characteristic couplings between initial instability and subsequent development of salt fingers have been studied systematically. In particular, this study provides an explanation for the mechanism of the generation of large-scale convective overturning of the flow in the reservoir, known phenomenologically as an onset to turbulence in the growth of double-diffusive salt fingers. The results of this study conclude that the phenomenon of salt fingers is fundamentally time dependent and unstable. Finally, this study is much motivated by the recent experimental results reported in Ref. [4].

The author is grateful to G. Veronis, J. Toomre, and C. Shen for their help in conducting the present work. This work was supported by a grant from the Korean Ministry of Science and Technology.

[1] H. Stommel, A. B. Arons, and D. Blanchard, Deep-Sea Res. **3**, 152 (1956).
[2] H. E. Huppert and J. S. Turner, J. Fluid Mech. **106**, 209 (1981).
[3] J. Taylor and G. Veronis, Science **231**, 39 (1986).
[4] J. Taylor and G. Veronis, J. Fluid Mech. **321**, 315 (1996).
[5] M. E. Stern, J. Fluid Mech. **35**, 209 (1969).
[6] J. Y. Holyer, J. Fluid Mech. **147**, 169 (1984).
[7] J. S. Turner, Annu. Rev. Fluid Mech. **17**, 11 (1985).
[8] S. A. Piacsek and J. Toomre, in *Marine Turbulence*, edited by J. C. T. Nihoul (Elseivier, New York, 1980), p. 193.
[9] C. Y. Shen, Phys. Fluids A **1**, 829 (1989).
[10] S. A. Orszag, Stud. Appl. Math **50**, 293 (1971).
[11] J. P. Christiansen, J. Comput. Phys. **13**, 363 (1973).
[12] J. Gazdag, J. Comput. Phys. **20**, 196 (1976).